Theor Chem Acc (2011) 128:147–155
DOI 10.1007/s00214-010-0834-3

FEATURE ARTICLE

Vibrational energy relaxation of small molecules and ions in liquids

J. L. Skinner

Received: 7 April 2010 / Accepted: 5 October 2010 / Published online: 24 October 2010

Abstract A theoretical/computational framework for determining vibrational energy relaxation rates, pathways, and mechanisms, for small molecules and ions in liquids, is presented. The framework is based on the system—bath coupling approach, Fermi's golden rule, classical time-correlation functions, and quantum correction factors. We provide results for three specific problems: relaxation of the oxygen stretch in neat liquid oxygen at 77 K, relaxation of the water bend in chloroform at room temperature, and relaxation of the azide ion anti-symmetric stretch in water at room temperature. In each case, our calculated lifetimes are in reasonable agreement with experiment. In the latter two cases, theory for the observed solvent isotope effects illuminates the relaxation pathways and mechanisms. Our results suggest several propensity rules for both pathways and mechanisms.

Keywords Vibrational relaxation · Liquids

1 Introduction

Consider a small molecule, with vibrational quantum states labeled i, in a liquid. In thermal equilibrium, the probability of finding the molecule in state i is given by the Boltzmann factor $P_i = e^{-\beta E_i}/Z$, where E_i is the energy of the ith state, $\beta = 1/kT$, and Z is the vibrational partition function. Suppose that at some time $t = 0$ the system is perturbed from equilibrium. Thus, if the non-equilibrium probability of finding the molecule in state i is defined to be $P_i(t)$, in general, $P_i(0) \neq P_i$. As time evolves, the system will relax to equilibrium, such that $P_i(\infty) = P_i$. The question is, what are the $P_i(t)$, for $0 \leq t \leq \infty$? This is the problem of vibrational "population" relaxation. Since as the vibrational populations relax, so does the vibrational energy, this process is also called vibrational energy relaxation (VER) [1–11].

One cares about VER because it is intimately related to chemical reactions. In a typical reaction, some chemical bonds are formed while others are broken. Bonds are broken after sufficient vibrational excitation, while bonds are formed as a result of vibrational relaxation. Thus, the rates, mechanisms, pathways, and branching ratios of thermal and laser-induced chemical reactions are determined by the rates of vibrational excitation and relaxation. In particular, the possibility of mode-selective chemistry depends crucially on VER rates not being too fast [12–14].

VER is typically measured experimentally with pump-probe transient absorption spectroscopy. That is, a molecule is perturbed from vibrational equilibrium, typically with an infrared pump laser, and then the populations of the various vibrational levels are measured at variable delay times through the transient absorption of an infrared probe laser. Often the pump laser excites a particular vibrational transition. The probe laser can monitor the same transition (in a one-color experiment), or different transitions (in a multi-color experiment). In an ingenious and powerful variant, one can also monitor, simultaneously, populations of several levels using anti-Stokes Raman probing [15].

The simplest theoretical approach to understanding VER is through the phenomenological "master equation", [16] which represents first-order kinetics for the non-equilibrium populations $P_i(t)$:

J. L. Skinner (✉)
Theoretical Chemistry Institute and Department of Chemistry, University of Wisconsin, Madison, WI 53706, USA
e-mail: skinner@chem.wisc.edu

$$\dot{P}_i(t) = -\sum_j k_{ij} P_i(t) + \sum_j k_{ji} P_j(t), \quad (1)$$

where k_{ij} is the rate constant for making a transition from state i to state j. $k_{ii} \equiv 0$, and the rate constants must obey detailed balance: $k_{ij} P_i = k_{ji} P_j$. The master equation can be solved in a straightforward manner subject to an initial condition. The resulting solution involves multi-exponential decay to equilibrium. In special cases, like the two-state approximation, or in the case of a harmonic oscillator linearly coupled to a bath, relaxation to equilibrium is strictly exponential [17, 18]. In experiments, rather than measuring the multi-exponential decay to equilibrium, often one can measure specific rate constants or sums of rate constants. For example, the "lifetime" T_i of a particular vibrational state i is given by $1/T_i = \sum_j k_{ij}$.

The simplest theoretical approach to calculating the rate constants k_{ij} involves system—bath coupling. Therein, the "system" is chosen to be the vibrational Hamiltonian for the molecule of interest, and the "bath" involves all the other nuclear degrees of freedom (molecular translations, rotations, and vibrations of other molecules). The coupling between system and bath allows energy to flow between them and produces VER. One usually treats the coupling in perturbation theory with Fermi's golden rule, which in the time-dependent representation shows that the rate constant k_{ij} is the Fourier transform, at the frequency $\omega_{ij} = (E_i - E_j)/\hbar$, of the quantum time-correlation function (TCF) of the ij system matrix element of the coupling [18–56]. Several workers have also proposed methods that in one way or another go beyond lowest order in perturbation theory [48–50, 57–59]. Although there have been some recent efforts to provide an approximate evaluation of the quantum TCF, [33–41, 47] it is more convenient to replace it with a classical TCF, in which case the Fourier transform must be multiplied by a "quantum correction factor" [17, 60–70]. For any chemical problem, one must then choose how to model the system, the bath, and the coupling and choose the appropriate quantum correction factor. An alternative approach to calculating VER rates is to perform non-equilibrium (classical) simulations [70–80].

For any particular chemical problem, one would like to know the values of each rate constant. The relative values of these rate constants provide information about the relaxation *pathways*, that is, which vibrational levels the population passes through as the system loses energy to the bath and equilibrates. One also wants to understand the *mechanism* of VER, that is, into which solvent modes is the energy deposited? Varying the isotope of the solvent can often help unravel VER mechanisms. In this account, I will first outline some of the theoretical issues in VER calculations and then discuss three applications, to VER of neat liquid oxygen at 77 K, of the bend of water in liquid chloroform, and of the anti-symmetric stretch of azide anion in water. In each case, I will discuss pathways and mechanisms and compare to experiment.

2 Theoretical approaches

One sets up the problem by writing the Hamiltonian for the molecule of interest (solute) in a liquid solvent as

$$H = H_s + H_b + \Lambda, \quad (2)$$

where H_s (s for system) is the vibrational Hamiltonion for the solute, H_b (b for bath) is the Hamiltonian for all other nuclear degrees of freedom, and Λ is the coupling between system and bath. H_s has vibrational eigenstates and eigenvalues according to

$$H_s|i\rangle = E_i|i\rangle. \quad (3)$$

H_b involves the translational and rotational degrees of freedom of all molecules, as well as the vibrational degrees of freedom of the solvent. Note that H_s and H_b operate in completely distinct Hilbert spaces. The coupling operator Λ involves operators (only coordinates, typically) in both Hilbert spaces.

From Fermi's golden rule, one can show that [1, 2]

$$k_{ij} = \frac{1}{\hbar^2} \int_{-\infty}^{\infty} \mathrm{d}t \; e^{i\omega_{ij}t} \langle \Lambda_{ij}(t) \Lambda_{ij}^{\dagger}(0) \rangle, \quad (4)$$

where ω_{ij} is defined in the Introduction, $\Lambda_{ij} \equiv \langle i|\Lambda|j\rangle$ is the system matrix element of the Λ operator (and is therefore still a bath operator), the Heisenberg time dependence of any bath operator is given by $A(t) = e^{iH_b t/\hbar} A e^{-iH_b t/\hbar}$, and

$$\langle A \rangle \equiv \mathrm{Tr}_b[e^{-\beta H_b} A]/\mathrm{Tr}_b[e^{-\beta H_b}]. \quad (5)$$

Typically, $\Lambda_{ij} = \Lambda_{ij}^{\dagger} = \Lambda_{ji}$. Assuming this to be the case and defining the quantum TCF by

$$C_{ij}(t) = \langle \Lambda_{ij}(t) \Lambda_{ij}(0) \rangle, \quad (6)$$

and its Fourier transform by $\hat{C}_{ij}(\omega)$, one sees simply that

$$k_{ij} = \frac{1}{\hbar^2} \hat{C}_{ij}(\omega_{ij}). \quad (7)$$

From the general time symmetries of quantum TCFs, one can show that for the Fourier transform of any quantum TCF $\hat{C}(-\omega) = e^{-\beta\hbar\omega} \hat{C}(\omega)$. From this it follows that $k_{ji} = e^{-\beta\hbar\omega_{ij}} k_{ij}$, which is the detailed balance condition mentioned above [63].

This approach, then, provides a formally correct (within perturbation theory) route for obtaining VER rate constants. However, for a solute molecule in a liquid solvent, it is often not possible to calculate an accurate approximation to the above quantum TCF. On the other

hand, it is usually straightforward to calculate the TCF classically. We define the classical-bath approximation to the rate constant by

$$k_{ij}^{cl} = \frac{1}{\hbar^2}\hat{C}_{ij}^{cl}(\omega_{ij}), \tag{8}$$

where $\hat{C}_{ij}^{cl}(\omega)$ is the Fourier transform of the classical TCF analogous to the quantum TCF in Eq. (6). For a classical TCF $C^{cl}(t)$, its Fourier transform has the property that $\hat{C}^{cl}(-\omega) = \hat{C}^{cl}(\omega)$. From this, we see that $k_{ij}^{cl} = k_{ji}^{cl}$, which violates detailed balance (unless $\omega_{ij} = 0$). If $\hbar\omega_{ij}/kT \ll 1$ this is not a serious problem, as one makes only a small error through this approximation. If, however, $\hbar\omega_{ij}/kT \gg 1$, then this is a horrible approximation.

Suppose, for example, that one is considering VER in liquid nitrogen [54]. In particular, one would like to calculate k_{10} and k_{01} for transitions between the ground and first excited states. ω_{10} is 2,331 cm^{-1}, and so at 77 K $e^{\hbar\omega_{10}/kT} \simeq 10^{19}$, which means that k_{10} is 10^{19} times larger than k_{01}. Clearly, the classical-bath approximation is seriously in error! One might say, with some justification, that one only needs to calculate k_{10}, since k_{01} is so astronomically small. Even so, since the classical-bath approximation gets the rate constant *ratio* wrong by 19 orders of magnitude, it seems likely that it will also get the *value* of k_{10} wrong!

One way to deal with the problem is through quantum correction factors (QCFs) [17, 60–70]. In this approach, one approximates the Fourier transform of a quantum TCF, by the Fourier transform of the corresponding classical TCF times a QCF. There are a number of different possible QCFs, [63, 67] each of which is constructed using the exact time symmetries of quantum TCFs, and so, as such, they obey detailed balance. Even so, however, they are certainly not exact (except for particular model problems), and different QCFs can differ by orders of magnitude. We have made some attempt to suggest which QCFs are most appropriate for different physical circumstances [64]. Very roughly, our conclusion is that if one excites one quantum of intermolecular or intramolecular bath vibration during the VER process, one should use the "harmonic" QCF, while if one excites many bath quanta, the "harmonic/Schofield" QCF is more appropriate. More work needs to be done in order to understand the proper use of these QCFs. In any case, the approximation we will use herein is that

$$k_{ij} \simeq Q(\omega_{ij})k_{ij}^{cl}, \tag{9}$$

as described above. The harmonic QCF is given by

$$Q_H(\omega) = \frac{\beta\hbar\omega}{1 - e^{-\beta\hbar\omega}}, \tag{10}$$

and the harmonic/Schofield QCF is given by

$$Q_{HS}(\omega) = e^{\beta\hbar\omega/4}Q_H(\omega)^{1/2}. \tag{11}$$

3 Some examples

3.1 Neat liquid oxygen at 77 K

In this system, the solute and solvent are both oxygen molecules. We denote the ground vibrational state of each molecule by $i = 0$ and the first excited state by $i = 1$. Since $\beta\hbar\omega_{10} \gg 1$, in thermal equilibrium essentially all of the molecules are in their ground states. Experimentally, one can prepare the system with a dilute concentration of single excitations—that is, molecules in $i = 1$ [81]. These excitations can hop from molecule to molecule through resonant energy transfer, but this process has never been measured experimentally in oxygen. Moreover, while from the perspective of a *single* oxygen molecule this hopping process corresponds to VER, from the perspective of the ensemble no VER has occurred, since the ensemble still has the same number of vibrational excitations. Experimentally, one has measured the lifetime of $i = 1$ for the ensemble, involving the rate that vibrational excitations decay to the ground state, independent of which molecules they are on. The lifetime at 77 K is 2.5 ms, [81] and since (see above) $1/T_1 \simeq k_{10}$, this gives $k_{10} \simeq 395\,\text{s}^{-1}$. This is a very slow process indeed! Since the intermolecular hopping process is not relevant for these measurements, the VER mechanism must involve transfer of vibrational excitation into bath modes comprised of molecular rotation and translation [36, 51].

To address the problem theoretically, we first need to specify the system Hamiltonian. Since we are only interested in the lowest two vibrational states, and oxygen is quite harmonic, we simply take [54]

$$H_s = \frac{p^2}{2\mu} + \frac{kq^2}{2}, \tag{12}$$

where μ is the reduced mass, q is the internuclear distance with respect to its equilibrium value, p is the conjugate momentum, and k is the harmonic force constant. For this harmonic oscillator Hamiltonian, the transition frequency is of course given by $\omega_{10} = \sqrt{k/\mu}$, which for oxygen is 1,552 cm^{-1}.

Next, we discuss the bath Hamiltonian, which as described above, must include molecular translation and rotation. As discussed above, the bath is described classically. We choose a two-site Lennard-Jones model for the oxygen intermolecular potential, and we optimize the σ and ε parameters to get agreement with experimental pressure and internal energy data from 70 to 126 K [82]. We then test the model by considering two microscopic experiments: X-ray scattering, [83] which leads to the intermolecular radial distribution function, $g(r)$, and depolarized Raman scattering, [84] which measures the second-rank

rotational TCF $\phi_2(t) = \langle P_2(\cos\theta(t))\rangle$, where P_2 is the second Legendre polynomial and $\theta(t)$ is the angle between molecule-fixed unit vectors at times 0 and t. Comparison between theory (labeled 'new") and experiment [83, 84] for these two quantities are shown in Figs. 1 and 2. In both cases, the excellent agreement gives us some confidence in the model for the bath Hamiltonian. Note that in Fig. 1, the curve marked BLF comes from an earlier two-site Lennard-Jones model developed by Bohn, Lustig, and Fischer, [85], and the two curves marked short and long BLF in Fig. 2 come from the same model with two different choices for the positions of the masses [82].

The system—bath coupling term involves interactions between molecular vibration on one molecule, and the rotations and translations of all molecules (including the "tagged" one). Thus, we consider how the total energy changes if the tagged molecule is stretched or compressed [54]. First of all, as the bond length of the tagged molecule changes (keeping the center-of-mass fixed), so does the potential energy in the two-site Lennard-Jones model. Second, when the bond length changes so does the molecule's moment of intertia, which couples the vibration to the rotational kinetic energy of the same molecule. Finally, in principle, the Lennard-Jones parameters themselves (for the interaction between the tagged molecule and the others) depend on the tagged molecule's bond length, since the electronic structure of a diatomic molecule depends on its bond length, and the intermolecular σ and ε parameters are related to electronic structure. This latter quite subtle interaction was determined by comparing [86] theoretical Raman line shifts and widths, as a function of temperature along the coexistence line, to experiment.

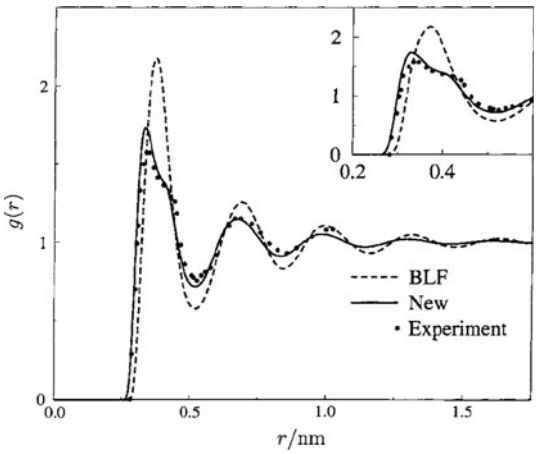

Fig. 1 Intermolecular radial distribution function for the site positions in liquid oxygen at 77 K and 1 atm pressure: simulation results for the BLF [85] and new [82] models, and experiment [83]. The *inset* emphasizes the shape of the first peak

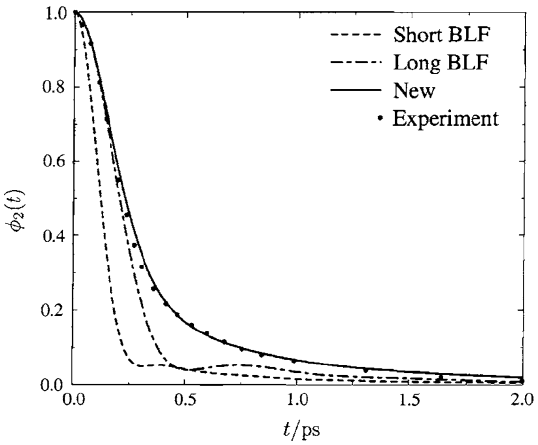

Fig. 2 Second-rank rotational time-correlation function for liquid oxygen at 77 K and 1 atm pressure: simulation results for the BLF [82, 85] and new [82] models, and experiment [84]

As described above, to calculate k_{10}, we need $C_{10}^{cl}(t)$. To this end, we expand Λ to first order in q:

$$\Lambda(q) \simeq \Lambda(0) + \left.\frac{\partial\Lambda}{\partial q}\right|_{q=0} q. \tag{13}$$

Defining the "force" (on the bond) by $F \equiv -\{\partial\Lambda/\partial q\}|_{q=0}$, we see that

$$C_{10}^{cl}(t) = q_{10}^2\langle F(t)F(0)\rangle. \tag{14}$$

Note that q_{10} is determined trivially for a harmonic oscillator, and F is a bath variable. Thus, the required classical force–force TCF can easily be calculated during the course of a classical molecular dynamics simulation for the bath.

The final specification we must make involves the QCF. As discussed above, for oxygen the VER process involves energy transfer from vibration to the rotations and translations of the bath. The characteristic frequencies of the latter on are the order of 50 cm^{-1}. That means the physical process involves the annihilation of one quantum of vibration, and the simultaneous creation of roughly thirty quanta of bath excitation. This is precisely the situation where we would advocate using the harmonic/Schofield QCF [64] (as the best choice among limited options).

The program described above was carried out for oxygen at 77 K, and the product of the Fourier transform of the classical TCF and the QCF is shown in Fig. 3 (labeled "Total"), as a function of frequency [54]. Also shown are the diagonal contributions (labeled B, K, and L) for the three components of the force, [54] as described above. Note that the largest contribution, B, comes from changes in the bond length [54]. Because of the substantial separation of time scales in this problem, the calculation of the Fourier transform is plagued by noise above about 600 cm^{-1}. But we need to evaluate this product at 1,552 cm^{-1}! The only way to proceed is to extrapolate our

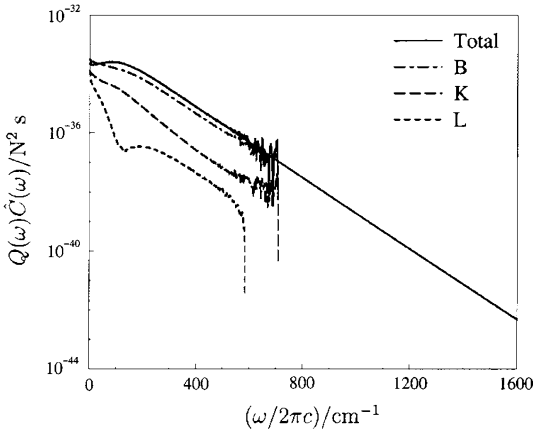

Fig. 3 The harmonic/Schofield quantum correction factor $Q(\omega)$ times the Fourier transform of the classical force–force TCF for liquid oxygen at 77 K (on a log plot), and the extrapolation to high frequencies [54]. Also shown are the diagonal contributions (labeled B, K, and L) for the three components of the force [54]. Note that the (non-negligible) cross-term contributions are not shown

results, using the reasonable exponential energy gap law, to higher frequencies, as shown in the figure [54].

Our theoretical result for the VER rate is $k_{10} = 1{,}100$ s^{-1}, which is about a factor of three larger than experiment. Although for some problems a factor of three disagreement with experiment might be considered an abject failure, for this problem we consider it a triumph! After all, one is trying to estimate the time scale for a process occurring in a few ms, when the characteristic time scale for molecular motion in a liquid is a few fs, thus bridging at least ten orders of magnitude. There are several sources of possible error, including the bath potential (to which the VER rate is quite sensitive), the system—bath coupling, and the QCF. Note, for example, that if one instead chooses the harmonic QCF, the rate is smaller by a factor of 261. For this problem, it is not really possible to know which is the source of the error; perhaps more likely, all are in error, and a fortuitous cancelation leads to a reasonable result.

3.2 Bend of water in liquid chloroform

Here, we consider VER of the bend vibration of dilute water in liquid chloroform at room temperature. The vibrations of the water molecule at low energy are very simple: the first two excited states are the bend fundamental and bend overtone. In the experiments to be discussed, the bend fundamental at roughly 1,600 cm^{-1} is excited with an infrared pump laser, and the vibrational lifetime $T_1 \simeq 1/k_{10}$ is measured. In normal liquid chloroform, the lifetime is found to be 8 ps, while in deutero-chloroform, the lifetime is 28 ps! [87]. This is a remarkably large solvent isotope effect, especially considering that substitution of H with D barely changes the molecular mass and moment of inertia, and hence the characteristic frequencies of solvent rotation and translation. On the other hand, deuteration does lead to large changes in some of the vibrational modes (see Table 1), strongly suggesting that the VER mechanism in this problem involves solute vibration to solvent vibration energy transfer [87].

As in the case of oxygen, since we are only interested in the first two vibrational states, a harmonic approximation is probably adequate, and so we use [56] the "rigid bender" Hamiltonian

$$H_s = \frac{L^2}{2I} + \frac{\gamma\theta^2}{2}, \tag{15}$$

where I is the angular momentum, θ is the HOH angle with respect to its equilibrium value, L is the conjugate angular momentum, and γ is the bending constant. The fundamental frequency is $\omega_{10} = \sqrt{\gamma/I} = 1{,}600\,\mathrm{cm}^{-1}$. For the bath Hamiltonian, since we anticipate that vibration–vibration energy transfer is an important mechanism, we need an accurate description of the solvent vibrations, for both normal and deuterated chloroform. For this, we turn to the Sibert-Rey model, [22] whose vibrational frequencies are compared with experiment in Table 1. As in the case with oxygen, the VER results are sensitive to the form of the solute/solvent potential. In this case, we found it necessary to develop [56] a new water/chloroform potential based on electronic structure calculations. For the system—bath coupling, for this problem we include only the simplest interaction that arises from the change in the nuclear positions of the hydrogen and oxygen atoms as the molecule bends, and the corresponding change in the water/chloroform potential energy.

Table 1 Fundamental frequencies, in cm^{-1}, of chloroform and deutero-chloroform, from experiment [94] and from the Sibert-Rey model [22]. The E modes are doubly degenerate

Symmetry	Mode	Description	Exp (H)	Model (H)	Exp (D)	Model (D)
A_1	ν_1	C–H(D) stretch	3,019	3,151	2,256	2,321
A_1	ν_2	C–Cl stretch	668	681	651	661
A_1	ν_3	Cl–C–Cl bend	366	377	367	374
E	ν_4	Cl–C–H(D) bend	1,216	1,240	908	923
E	ν_5	C–Cl stretch	761	786	738	759
E	ν_6	Cl–C–Cl bend	262	268	262	267

As in the previous example, to calculate $C_{10}^{cl}(t)$, we expand [56] Λ to first order in θ, and calculate the analogue of the classical force–force TCF. Regarding the appropriate QCF, the experiments indicate the likelihood of intermolecular vibration–vibration coupling, and there are some solvent vibrational modes that are relatively near-resonant with the water bend. Thus, it seems likely that a zeroth-order picture is that in the VER process one quantum of solvent vibration is created, suggesting that the harmonic QCF is the most appropriate choice. Our theoretical results [56] give a bend lifetime of 17 ps in chloroform (compared to 8 ps in experiment [87]), and 44 ps in deutero-chloroform (compared to 28 ps in experiment [87]). Thus, our lifetimes are somewhat too long, but the trend with isotopic substitution is correct. One possibility for the discrepancy with experiment is our neglect of the centrifugal coupling contribution to the force [56].

We can now go on to attempt to address two questions. The first involves the VER mechanism: into which bath modes is the energy deposited? To answer this question, we consider [56], in addition to the (fully-vibrating-solvent) simulation already performed, two more, where the C–Cl stretches are frozen, and where *all* solvent vibrations are frozen. In Fig. 4, we plot the Fourier transform of the classical TCF, for chloroform and deutero-chloroform, and for each of these three simulations. Recall that these need to be evaluated at a frequency of 1,600 cm^{-1}. First considering the upper panel for chloroform, when we freeze the C–Cl stretches (whose frequencies, from the table, are close to 700 or 800 cm^{-1}), we see that the value of the Fourier transform drops (from the "flexible" value), showing that these stretch modes are important accepting modes in the VER process. When we further freeze *all* the solvent vibrations, the value of the Fourier transform drops significantly again. Noting the presence in the "flexible" result of the strong peak at just over 1,200 cm^{-1}, corresponding to the C–Cl–H bend (see Table 1), it is most likely that these bend modes are responsible for the remaining drop. Thus, we conclude that the VER mechanism involves the transfer of one quantum of water bend excitation, into one quantum of C–Cl–H bend (and one or more quanta of lower-frequency modes), or one or more quantum of C–Cl stretches.

The second question involves the source of the interesting isotope effect. In the lower panel, we see that the peak for the C–Cl–D bend (now at about 900 cm^{-1}) is less pronounced. Thus, the water bend mode couples less strongly to this bend in the case of deutero-chloroform. In addition, the mode is now further off resonance, and so the difference between the values of the Fourier transforms in the flexible and rigid cases (the latter of which is nearly identical for the two isotopes, as discussed above) is smaller. Thus, we conclude that in the case of deutero-chloroform, the bend, being further off resonance, is less effective as an accepting mode, which is primarily responsible for the observed solvent isotope effect.

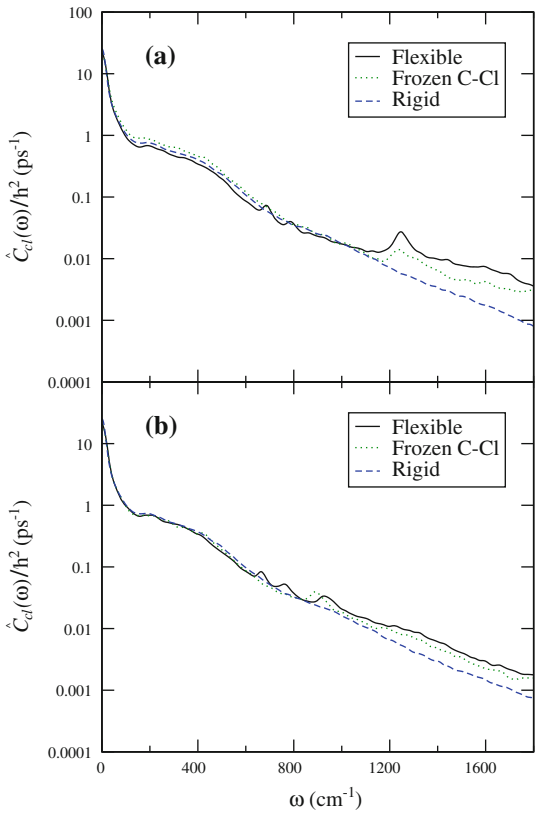

Fig. 4 Fourier transform of the relevant classical TCF for the water bend (on a log plot), at room temperature, in (**a**) chloroform, and (**b**) deutero-chloroform [56]. In each case, the three curves correspond to fully flexible chloroform solvent, chloroform with the C–Cl stretches frozen, and completely rigid chloroform

3.3 Anti-symmetric stretch of azide anion in water

The last example involves azide ion in water (and heavy water) at room temperature. The linear azide ion has four vibrational normal modes—two degenerate bends (at about 700 cm^{-1}), the symmetric stretch at about 1,300 cm^{-1}, and the anti-symmetric stretch at about 2,000 cm^{-1}. In the relevant experiments, the fundamental of the anti-symmetric stretch mode is excited, and its vibrational lifetime is found to be about 1 ps in water, and 2.3 ps in heavy water [88–90]. For this problem, there are three interesting questions to address: [21, 55] (1) what is the dominant VER pathway (to the symmetric stretch fundamental, the various bend modes, or directly to the ground state)? (2) what is the VER mechanism (into which solvent modes is the energy deposited)? (3) what is responsible for the observed solvent isotope effect? Note that in this case

isotope substitution in water from H to D *does* significantly change the moment of inertia, and hence the librational frequencies. It also, of course, changes the water bend and stretch frequencies.

In order to choose H_s, we first note that gas-phase spectroscopy indicates that the azide bends and stretches are only weakly coupled [91]. Since the molecule initially has a stretch excitation, in the simplest scenario only stretches will be important during the VER process. Thus, we assume that a two-dimensional stretch-only model will suffice [55, 92, 93]. It is most convenient to formulate the model as two coupled local-mode Morse oscillators, the parameters of which are determined from electronic structure calculations [92].

In order to model the bath, we need to presuppose a relaxation pathway and mechanism. For example, if the pathway is direct relaxation to the ground state, the water bend vibrations could function as accepting modes, in which case we would need a model with flexible water. On the other hand, if the pathway is relaxation to the azide symmetric stretch, with a gap of about 700 cm^{-1}, it is unlikely that the higher-frequency bend vibrations play a role, and so a rigid water model would suffice. The general thinking in this field is that the dominant pathways typically involve relatively small gaps, and so the latter scenario seems more likely. Assuming this to be the case, our model of the bath involves rigid linear azide ion in a solvent composed of rigid water molecules.

As in the previous example, we take the system–bath coupling to arise only from potential energy interactions. As before, we expand the system–bath coupling in powers of the relevant coordinates (in this case, the *two* local-mode coordinates), only here we need to go to second order in the expansion. In order to determine the coefficients in the expansion, we examined several approaches, the most promising of which involves an optimized QM/MM (quantum mechanics/molecular mechanics) procedure [55, 92, 93].

The gap between the anti-symmetric and symmetric stretch states is roughly 700 cm^{-1}. In order to choose the QCF, in principle we need some information on the VER mechanism—which solvent modes are excited. Two possibilities are the hydrogen-bond stretching mode in water at about 250 cm^{-1}, and the water libration (at about 600 cm^{-1} in heavy water and 800 cm^{-1} in water). In the case of the former, about three quanta of excitation would be created, and so one should probably choose [64] the harmonic/Schofield QCF, while in the case of the latter only one quanta would be created, and so the harmonic QCF would be more appropriate. In fact, however, for relatively small gaps at relatively high temperature, as in this case, it does not make too much difference which QCF we choose, and so we went with the harmonic/Schofield QCF.

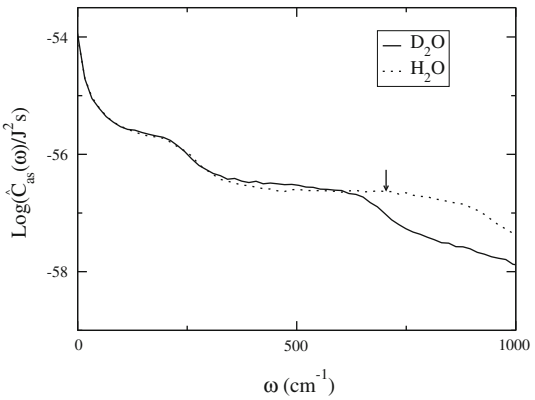

Fig. 5 Fourier transform of the relevant classical TCF for azide anion at room temperature, in both H_2O and D_2O [55]. The *arrow* indicates the transition frequency for the anti-symmetric to symmetric stretch energy gap

Our results [55] for this problem give an anti-symmetric stretch lifetime of 0.96 ps in water, and 2.7 ps in heavy water (compared to the experimental values of 1 and 2.3 ps, respectively). This good agreement with experiment suggests that the assumptions we have made about this system are probably correct, and that, for example, the dominant VER pathway is to the symmetric stretch fundamental. To understand both the mechanism and the solvent isotope effect, in Fig. 5 we show the Fourier transform of the relevant classical TCF for azide in both water and heavy water. Recall that these need to be evaluated at about 700 cm^{-1}. For heavy water, this frequency is just to the blue of the plateau due to solvent libration, while in normal water is in the middle of the librational plateau. Thus, in water it is clear that the libration is the accepting mode. It is equally clear that in this case the solvent isotope effect arises because the librational frequency in heavy water is shifted just to the red of the gap frequency, and so this libration functions less well as an accepting mode.

4 Concluding remarks

In this review, I have outlined a theoretical/computational framework for calculating the rates, pathways, and mechanisms of vibrational energy relaxation for small molecules and ions in liquids. The framework involves the system–bath coupling approach, Fermi's golden rule, the calculations of appropriate classical time-correlation functions, and quantum correction factors. For a specific problem of a solute in a liquid solvent, the appropriate approaches to model the system and bath are determined in part by assumptions as to the relaxation pathway and mechanism. That is, one needs to make assumptions about the relevant

vibrational quantum states of the solute, and the relevant accepting modes of the bath. The modeling of the system, bath, and coupling Hamiltonian can be made at different levels of sophistication, from using empirical energy surfaces, to detailed electronic structure calculations. The choice of the most appropriate quantum correction factor is also dependent on some assumptions about the relaxation pathway and mechanism.

From the above, it is clear that such vibrational relaxation calculations are not completely straightforward, and the results are not completely unambiguous. Still, with thoughtful consideration of the chemical systems, and careful choice of the appropriate level of modeling the Hamiltonian, one can obtain semi-quantitative agreement with experiment, and probably more importantly, can determine relaxation pathways and mechanisms.

I considered three specific examples herein: oxygen stretch in neat liquid oxygen, bend of water in chloroform, and anti-symmetric stretch of azide in water. In all three cases, relaxation appears to proceed to the nearest vibrational level (which could be the ground state) below the initially excited vibrational state. The solvent accepting modes are those most nearly resonant with the solute energy gap. Thus, in oxygen, there are no near-resonant modes, and so the process is very slow (on the order of a ms). For the azide problem, there are near-resonant modes—the water libration—and so the relaxation is very fast (on the order of a ps). For the water relaxation in chloroform problem, there are no very-near-resonant solvent modes, but there are modes not so far off resonance, and so relaxation is somewhat slower (with times on the order of 10–30 ps) than in the azide case, but much faster than in the oxygen case. The "order" of the process is clearly concomitant with the resonance (or lack thereof) with solvent modes, and hence the speed of the process. Thus, in oxygen one must create roughly 30 quanta of solvent excitation, for water in chloroform one must create at least two, and for azide in water a single quantum suffices. For the water and azide VER problems, one can understand the interesting solvent isotope effects from considering how the solvent vibrational or librational frequencies move closer to or farther from resonance with the solute energy gap. Such propensities may hold more generally for other systems.

On the experimental side, studies on a wider range of systems would be very helpful. As for theory, more work needs to be done in developing accurate model potentials, understanding more fully how to use quantum correction factors appropriately, or better yet, developing alternative quantum procedures that obviate their need.

Acknowledgments This article is based on a series of lectures I gave in Jyväskylä Finland in 2007, which in turn was based on a portion of my advanced statistical mechanics course at the University of Wisconsin. I thank Mika Pettersson for inviting me to give the lectures, and various generations of graduate students for enduring my course. The three chemical examples come from my own research, in collaboration with Karl Everitt, Branka Ladanyi, Shuzhou Li, J. R. Schmidt, Yu-Shan Lin, Sai Ramesh, Justin Shorb, and Ned Sibert, to all of whom I am indebted. This research is supported by NSF (CHE-0750307) and DOE (DE-FG02-09ER16110).

References

1. Oxtoby DW (1981) Adv Chem Phys 47(Part 2):487
2. Oxtoby DW (1983) J Phys Chem 87:3028
3. Harris CB, Smith DE, Russell DJ (1990) Chem Rev 90:481
4. Owrutsky JC, Raftery D, Hochstrasser RM (1994) Annu Rev Phys Chem 45:519
5. Stratt RM, Maroncelli M (1996) J Phys Chem 100:12981
6. Okazaki S (2001) Adv Chem Phys 118:191
7. Skinner JL, Egorov SA, Everitt KF (2001) Vibrational energy relaxation in liquids and supercritical fluids. In: Fayer M (ed) Ultrafast Infrared and Raman Spectroscopy. Marcel Dekker, New York, pp 675
8. Stratt RM (2001) The molecular mechanisms behind the vibrational population relaxation of small molecules in liquids. In: Fayer M (ed) Ultrafast Infrared and Raman Spectroscopy. Marcel Dekker, New York, pp 149
9. Iwaki LK, Deàk JC, Rhea ST, Dlott DD (2001) Vibrational energy redistribution in polyatomic liquids: Ultrafast ir-raman spectroscopy. In: Fayer M (ed) Ultrafast Infrared and Raman Spectroscopy. Marcel Dekker, New York, pp 541
10. Myers DJ, Shigeiwa M, Fayer MD, Cherayil BJ (2001) Vibrational relaxation of polyatomic molecules in supercritical fluids and the gas phase. In: Fayer M (ed) Ultrafast Infrared and Raman Spectroscopy. Marcel Dekker, New York, pp 625
11. Rey R, Møller KB, Hynes JT (2004) Chem Rev 104:1915
12. Crim FF (1996) J Phys Chem 100:12725
13. Crim FF (1999) Acc Chem Res 32:877
14. Zare RN (1998) Science 279:1875
15. Deàk JC, Rhea ST, Iwaki LK, Dlott DD (2000) J Phys Chem A 104:4866
16. Oppenheim I, Shuler KE, Weiss GH (1977) Stochastic processes in chemical physics: the master equation. MIT Press, Cambridge
17. Bader JS, Berne BJ (1994) J Chem Phys 100:8359
18. Egorov SA, Skinner JL (1996) J Chem Phys 105:7047
19. Whitnell RM, Wilson KR, Hynes JT (1990) J Phys Chem 94:8625
20. Rey R, Hynes JT (1996) J Chem Phys 104:2356
21. Morita A, Kato S (1998) J Chem Phys 109:5511
22. Sibert EL, Rey R (2002) J Chem Phys 116:237
23. Gulmen TS, Sibert EL (2004) J Phys Chem A 108:2389
24. Ramesh SG, Sibert EL (2006) J Chem Phys 124:234501
25. Zhang FS, Lynden-Bell RM (2003) J Chem Phys 119:6119
26. Chorny I, Vieceli J, Benjamin I (2002) J Chem Phys 116:8904
27. Vieceli J, Chorny I, Benjamin I (2002) Chem Phys Lett 364:446
28. Li S, Thompson WH (2003) J Phys Chem A 107:8696
29. Li S, Thompson WH (2004) Chem Phys Lett 383:326
30. Li S, Shepherd TD, Thompson WH (2004) J Phys Chem A 108:7347
31. Miller DW, Adelman SA (2002) J Chem Phys 117:2672
32. Miller DW, Adelman SA (2002) J Chem Phys 117:2688
33. Poulsen JA, Rossky PJ (2001) J Chem Phys 115:8014
34. Poulsen JA, Rossky PJ (2001) J Chem Phys 115:8024
35. Shi Q, Geva E (2003) J Phys Chem A 107:9059
36. Shi Q, Geva E (2003) J Phys Chem A 107:9070

37. Shi Q, Geva E (2003) J Chem Phys 119:9030
38. Ka BJ, Shi Q, Geva E (2005) J Phys Chem A 109:5527
39. Ka BJ, Geva E (2006) J Phys Chem A 110:9555
40. Ka BJ, Geva E (2006) J Phys Chem A 110:13131
41. Navrotskaya I, Geva E (2007) J Phys Chem A 111:460
42. Ma A, Stratt RM (2003) J Chem Phys 119:6709
43. Ma A, Stratt RM (2004) J Chem Phys 121:11217
44. Ladanyi BM, Stratt RM (1999) J Chem Phys 111:2008
45. Deng Y, Stratt RM (2002) J Chem Phys 117:1735
46. Deng Y, Ladanyi BM, Stratt RM (2002) J Chem Phys 117:10752
47. Rabani E, Reichman DR (2001) J Phys Chem B 105:6550
48. Lawrence CP, Skinner JL (2002) J Chem Phys 117:5827
49. Lawrence CP, Skinner JL (2003) J Chem Phys 119:1623
50. Lawrence CP, Skinner JL (2003) J Chem Phys 119:3840
51. Everitt KF, Egorov SA, Skinner JL (1998) Chem Phys 235:115
52. Everitt KF, Skinner JL (1999) J Chem Phys 110:4467
53. Egorov SA, Skinner JL (2000) J Chem Phys 112:275
54. Everitt KF, Skinner JL, Ladanyi BM (2002) J Chem Phys 116:179
55. Li S, Schmidt JR, Skinner JL (2006) J Chem Phys 125:244507
56. Lin Y-S, Ramesh SG, Shorb JM, Sibert EL, Skinner JL (2008) J Phys Chem B 112:390
57. Bakker HJ (2004) J Chem Phys 121:10088
58. Gulmen TS, Sibert EL (2005) J Phys Chem A 109:5777
59. Ramesh SG, Sibert EL (2006) J Chem Phys 125:244512
60. Schofield P (1960) Phys Rev Lett 4:239
61. Skinner JL (1997) J Chem Phys 107:8717
62. Egorov SA, Skinner JL (1998) Chem Phys Lett 293:469
63. Egorov SA, Everitt KF, Skinner JL (1999) J Phys Chem A 103:9494
64. Skinner JL, Park K (2001) J Phys Chem B 105:6716
65. Lawrence CP, Nakayama A, Makri N, Skinner JL (2004) J Chem Phys 120:6621
66. Kim H, Rossky PJ (2002) J Phys Chem B 106:8240
67. Ramirez R, Lopez-Ciudad T, Kumar P, Marx D (2004) J Chem Phys 121:3973
68. Kim H, Rossky PJ (2006) J Chem Phys 125:074107
69. Kim H, Rossky PJ (2006) J Chem Phys 125:066101
70. Stock G (2009) Phys Rev Lett 102:118301
71. Brown JK, Harris CB, Tully JC (1988) J Chem Phys 89:6687
72. Whitnell RM, Wilson KR, Hynes JT (1992) J Chem Phys 96:5354
73. Jang S, Pak Y, Voth GA (1999) J Phys Chem A 103:10289
74. Käb G, Schröder C, Schwarzer D (2002) Phys Chem Chem Phys 4:271
75. Nguyen PH, Stock G (2003) J Chem Phys 119:11350
76. Ramesh SG, Sibert EL (2006) J Chem Phys 125:244513
77. Bastida A, Zúñiga J, Requena A, Miguel B (2008) J Chem Phys 129:154501
78. Kandratsenka A, Schroeder J, Schwarzer D, Vikhrenko VS (2009) J Chem Phys 130:174507
79. Ingrosso F, Rey R, Elsaesser T, Hynes JT (2009) J Phys Chem A 113:6657
80. Rey R, Ingrosso F, Elsaesser T, Hynes JT (2009) J Phys Chem A 113:8949
81. Faltermeier B, Protz R, Maier M (1981) Chem Phys 62:377
82. Perng B-C, Sasaki S, Ladanyi BM, Everitt KF, Skinner JL (2001) Chem Phys Lett 348:491
83. Furomoto HW, Shaw CH (1964) Phys Fluids 7:1026
84. Bruining J, Clarke JHR (1976) Mol Phys 31:1425
85. Bohn M, Lustig R, Fischer J (1986) Fluid Phase Equilibr 25:251
86. Everitt KF, Skinner JL (2001) J Chem Phys 115:8531
87. Seifert G, Patzlaff T, Graener H (2004) J Chem Phys 120:8866
88. Li M, Owrutsky J, Sarisky M, Culver JP, Yodh A, Hochstrasser RM (1993) J Chem Phys 98:5499
89. Hamm P, Lim M, Hochstrasser RM (1998) Phys Rev Lett 81:5326
90. Zhong Q, Baronavski AP, Owrutsky JC (2003) J Chem Phys 118:7074
91. Polak M, Gruebele M, Peng GS, Saykally RJ (1988) J Chem Phys 89:110
92. Li S, Schmidt JR, Piryatinski A, Lawrence CP, Skinner JL (2006) J Phys Chem B 110:18933
93. Li S, Schmidt JR, Corcelli SA, Lawrence CP, Skinner JL (2006) J Chem Phys 124:204110
94. Herzberg G (1950) Molecular spectra and molecular structure. II. Infrared and Raman spectra of polyatomic molecules. Van Nostrand, New York